# CISLUNAR METEOROID IMPACT AND PUNCTURE MODELS WITH PREDICTED PEGASUS SATELLITE PUNCTURES

by CHARLES C. DALTON
    Aero-Astrodynamics Laboratory

**NASA**

*George C. Marshall*

*Space Flight Center,*

*Huntsville, Alabama*

# CISLUNAR METEOROID IMPACT AND PUNCTURE MODELS WITH PREDICTED PEGASUS SATELLITE PUNCTURES

By

Charles C. Dalton

George C. Marshall Space Flight Center

Huntsville, Alabama

## ABSTRACT

*17541*

The author's previous model for the variation of meteoroid impact flux with respect to distance from the earth in cislunar space is simplified and corrected for the increase in the inferred mass of a meteoroid due to the new pressure values in the U. S. Standard Atmosphere, 1962. A new model for the corresponding puncture flux is developed as a function of material parameters and thickness by interpreting Explorer XVI puncture data in relation to the revised model for impact flux and to extrapolated results from the Martin Company's multivariate analysis of laboratory hypervelocity impact data.

During one year after a Pegasus satellite has been deployed in an orbit with perigee and apogee heights of 505 and 740 kilometers, the number of punctures in the 16 sheets of the 0.0015-inch sensor, the 34 sheets of the 0.008-inch sensor, and the 366 sheets of the 0.016-inch sensor are predicted to be approximately 5430, 41, and 38, respectively, when the extra material in the bonded capacitors is considered. The estimated masses of the meteoroids which can just puncture these sensors when they have the mean values of density (0.44 gram per cubic centimeter), velocity (26.7 kilometers per second), and impact angle ($\pi/4$ radian) are $10^{-7.84}$, $10^{-5.85}$, and $10^{-4.98}$ gram.

*Author*

NASA - GEORGE C. MARSHALL SPACE FLIGHT CENTER

NASA - GEORGE C. MARSHALL SPACE FLIGHT CENTER

Technical Memorandum X-53187

January 13, 1965

CISLUNAR METEOROID IMPACT AND PUNCTURE MODELS WITH
PREDICTED PEGASUS SATELLITE PUNCTURES

By

Charles C. Dalton

AERO-ASTROPHYSICS OFFICE
AERO-ASTRODYNAMICS LABORATORY

ACKNOWLEDGEMENTS

TABLE OF CONTENTS

## DEFINITION OF SYMBOLS

| Symbol | Definition |
|--------|------------|
| $F_s$ | mean total number of impacts of meteoroids, with mass equal to or greater than $m$ grams, per second per square meter of total area of a spherical vehicle or of a randomly oriented vehicle |
| $m$ | meteoroid mass in grams |
| $h$ | distance from the surface of the earth in kilometers |
| $\beta_2$ | slope of the line relating $\log F_s$ with $\log m$ at fixed distance $h$ |
| $\beta_3$ | intercept of the line relating $\log F_s$ with $\log m$ at fixed distance $h$ |
| $\rho_p$ | meteoroid material density in grams per cubic centimeter |
| $h_B$ | meteor height in kilometers above sea level at the point of appearance |
| $h_e$ | meteor height in kilometers above sea level at the point of disappearance |
| $Z$ | zenith angle to meteor radiant in radians |
| $v$ | meteoroid velocity before deceleration in the atmosphere |
| $M_p$ | meteor absolute photographic magnitude |
| $f$ | weighting function to reduce bias in photographic meteor data |
| $h_m$ | meteor height above sea level at the point of maximum brilliance. |
| $P$ | Öpik's probability that a meteoroid in a given orbit will encounter the earth during one revolution of the particle |
| $f_f$ | reciprocal of the apparent fraction of the circle of celestial latitude through the meteor radiant |
| $h_p$ | perigee height in kilometers above sea level |

## DEFINITION OF SYMBOLS

| Symbol | Definition |
|---|---|
| $h_a$ | apogee height in kilometers above sea level |
| $\bar{F}_s$, $\bar{\beta}_2$ | mean values of $F_s$ and $\beta_2$ around an orbit |
| $x_2$ | angle of impact in radians with respect to the normal |
| $\rho_t$ | target material density in grams per cubic centimeter |
| $H_t$ | target hardness in Brinell units |
| $p$ | thickness of the punctured wall in centimeters |
| $P_m$ | puncture probability for a meteoroid of mass m |
| $\emptyset$ | puncture flux; number per square meter per second |
| $\emptyset_1$, $\emptyset_2$ | puncture flux expected through 1-mil and 2-mil targets, respectively, on Explorer· XVI |
| $\bar{m}_1$, $\bar{m}_2$ | mass of meteoroids which, at mean density, mean velocity, and mean impact angle, would just puncture the 1-mil and 2-mil targets, respectively, on Explorer XVI |
| $P_o$ | crater depth in thick targets, centimeters |
| $d$ | projectile diameter in centimeters |
| $t$ | Target subscript |
| $C_t$ | bulk velocity of sound in kilometers per second |
| $Q$ | heat to melt in calories per gram |
| $E$ | $10^{-6}$ x Young's modulus, kilograms per square centimeter |
| $\epsilon$ | ductility, percent elongation in 2-inch gauge length at fracture |
| $Y$ | yield strength at 0.2 percent offset, kilograms per square centimeter |
| $\nu$ | Poisson's ratio |

TECHNICAL MEMORANDUM X-53187

# CISLUNAR METEOROID IMPACT AND PUNCTURE MODELS WITH PREDICTED PEGASUS SATELLITE PUNCTURES

## SUMMARY

In cislunar space at a distance of h kilometers from the surface of the earth, where $2 \leq \log h \leq 6$, the mean meteoroids $F_s$ with mass equal to or greater than m grams, where $-10 \leq \log m \leq 0$, impacting per second per square meter of total area of a randomly oriented orbiting vehicle should be considered to be an exponential function of m,

$$F_s = 10^{-14.92} \, m^{\beta_2},$$

where the exponent $\beta_2$ is a function of h:

$$\beta_2 = -1 - 0.34 e^{0.26(\log h - 2)} + 0.24(\log h - 2).$$

Correspondingly, the puncture flux $\emptyset$ through a homogeneous metallic wall of thickness p centimeters should be considered to be an exponential function of the nominally puncturing mass $\bar{m}$ with the same exponent $\beta_2$

$$\emptyset = 10^{-14.32} \bar{m}^{\beta_2},$$

where the nominally puncturing mass $\bar{m}$ is a function of the material parameters of the metallic wall:

$$\bar{m} = 10^{10.985} \, (p C_t^{0.50} \, E_t^{1.31} \, \nu_t^{8.0} \, \epsilon_t^{0.43})^3,$$

where $C_t$ is the bulk velocity of sound (kilometers per second), $E_t$ is $10^{-6}$ times Young's modulus (kilograms per square centimeter), $\epsilon_t$ is the ductility (percent elongation in 2-inch gauge length at fracture), and $\nu_t$ is Poisson's ratio.

During one year after a Pegasus satellite has been deployed in an orbit with perigee and apogee heights of 505 and 740 kilometers,* the number of punctures in the 16 sheets of the 0.0015-inch sensor, the 34 sheets of the 0.008-inch sensor, and the 366 sheets of the 0.016-inch sensor are predicted to be approximately 5430, 41, and 38, respectively,* when the extra material in the bonded capacitors is considered. The estimated masses of the meteoroids which can just puncture these sensors when they have the mean values of density (0.44 gram per cubic centimeter), velocity (26.7 kilometers per second), and impact angle ($\pi/4$ radian) are $10^{-7.84}$, $10^{-5.85}$, and $10^{-4.98}$ gram.

---

*See footnotes on page 19.

# I. INTRODUCTION

During the first half of 1964 Dalton [1] constructed a model which gave meteoroid impact and puncture flux as functions of the distance from the earth in cislunar space. The impact model was made to agree with Whipple's [2] near the earth, and the dependence on distance from the earth was given in consideration of arguments by Whipple [3], Hawkins [4], Briggs [5], and McCracken and Dubin [6]. Some changes in the impact flux involving both mass and velocity are introduced, but the main change from Reference 1 is that Dalton's [7] puncture model is revised in consideration of Hasting's [8, 9] data for Explorer XVI and the multivariate analysis of laboratory hypervelocity data by Reismann, Donahue, and Burkitt [10].

The earth shielding factor is included in the model; but no consideration is given to shielding by the moon, or to any secondary flux which may be encountered near the moon or on the lunar surface due to high velocity ejecta possibly initiated by the impact of meteoroids. The model is intended for present design considerations throughout ten orders of magnitude below meteoroid unit mass in grams and from one hundred to one million kilometers from the earth. All logarithms are for base ten. Errors representing uncertainty are roughly normally distributed, and the indicated probable errors represent a revision of the author's [1, 7] previous estimates due to a revised treatment with respect to density in Section V.

# II. FLUX ADJUSTMENT FOR NEW STANDARD ATMOSPHERE

Öpik [11] showed that meteor luminous efficiency is inversely proportional to the cube of the atmospheric pressure at the point of disappearance of the meteor. Dalton's [1] model presupposed Whipple's [2] model, which was based on the ARDC Model Atmosphere 1959 [12]. Three times the logarithm of the ratio of the means of the 85-90 kilometer pressure from the U. S. Standard Atmosphere 1962 [13] and the ARDC Model Atmosphere 1959 [12] gives a mass increment of 0.20 orders of magnitude. This corresponds to a flux increment of (1.34)(0.20) = 0.27 order of magnitude.

# III. FLUX ADJUSTMENT FOR MEAN SHOWER ACTIVITY

Whipple's [2] model was obtained by re-estimating the mass of the zero-visual-magnitude meteor in the model by Hawkins and Upton [14] for the flux of photographic meteors not belonging to the major streams (showers). Photographic data with similar limiting sensitivity were published by Hawkins and Southworth [15] who tabulated 74 shower and 286 sporadic meteors. In referring to this work of Hawkins and Southworth [15], Whipple and

Hawkins [16] indicated that 83 percent of such meteors do not belong to major streams. Therefore, a model for the mean total flux would seem to be obtained by increasing the mean flux for sporadic meteors by 0.08 order of magnitude; i.e., -log 0.83 = 0.08.

## IV. MEAN TOTAL IMPACT FLUX

By combining the increments indicated in Sections II and III, the impact flux in Dalton's [1] model is increased by 0.35 order of magnitude throughout cislunar space; i.e.,

$$\log F_s = \beta_2 \log m + \beta_3 \qquad (1)$$

$$\beta_2 = -\left[1 + 0.34 \ e^{0.26(\log h - 2)} - 0.24(\log h - 2)\right] \qquad (2)$$

$$\beta_3 = -14.2 \pm 0.60, \qquad (3)$$

where $F_s$ is the mean total number of impacts of meteoroids with mass equal to or greater than m grams per second per square meter of total area of a spherical vehicle or of a randomly oriented vehicle, and h is the distance from the surface of the earth in kilometers. The following approximation was made for a term in equation (3):

$$-0.028(\log h - 2) \simeq -0.07 \quad \text{for } 2 \leq \log h \leq 6$$

where the exact value of the term varies between 0 at log h = 2 and -0.10 at log h = 5.59 (lunar distance). The maximum error (near the earth) due to this approximation is small in comparison with the uncertainty in equation (3).

## V. MATERIAL DENSITY OF METEOROIDS

At the moon's distance from the earth, where the value of log h is 5.59, the slope $\beta_2$ in equations (1) and (2) has a unit negative value, and both $\beta_2$ and $\beta_3$ have the same values when the same units are used in Hawkins' [4] formula for the flux of large stone meteorites onto the earth. The presence of some stone meteoroids with mass less than one gram would not be too controversial.

Briggs [5] found that zodiacal-light observations are consistent with the theoretical apparent brightness due to scattered light from the steady-state system of particles in the solar system under the action of the Poynting-Robertson effect when it was assumed (1) that the concentration of particles with radii equal to or greater than 50 microns is inversely proportional to mass m at a distance of one astronomical unit from the sun (although not necessarily near the earth), and (2) that the material density is 0.1 for the larger particles (-7.3 < log m). The presence of a mixed population of particles, about 90 percent with density 0.1 and about 10 percent with the density of stone - Öpik [17] gives the density of meteoritic stone as 3.4 - would therefore not be surprising. The density 0.44 in Whipple's [2] model is approximately the mean density for such a mixed population of stones and dustballs, presumably derived from asteroids and comets, respectively. But the likelihood for such a mixed population has been discounted considerably in studies of photographic meteor data (for which approximately: $-2 \leq \log m \leq 1$) by Whipple and Hawkins [16], and by Jacchia and Whipple [18].

In Briggs' [5] model for small particles, discussed above, density $\rho_p$ increases from 0.1 through 0.44 as log m decreases from -7.3 through -9.5. Any tendency for small dustballs to approach the density of smaller constituent dust grains would not be surprising.

Evidently, the density is not very well known, but for present purposes the assumption of an effectively homogeneous population of particles, half of which have densities which do not differ by more than a factor between 1/2 and 2 from the mean density, and mean density equal to that in Whipple's [2] model to within a factor 2 probable error, seems to be a reasonable expedient; i.e.,

$$\log \rho_p = \log \bar{\rho}_p \pm 0.30$$

$$\log \bar{\rho}_p = -0.35 \pm 0.30 = \log 0.44 \pm 0.30$$

$$(4)$$

Only the uncertainty in the mean density appears to affect the uncertainty in the mean flux, and the author's [1, 7] previous estimates of uncertainty must be revised here.

4

## VI. METEOROID IMPACT VELOCITY

Dalton's [7] results show that meteoroids impact against an orbiting vehicle with very nearly the same mean impact speed as they have with respect to the atmosphere. For the present purpose, it seems appropriate to assume that the orbital velocity of the vehicle does not appreciably enhance either the flux or the closing velocity.

Because meteoroid mass ranges through ten orders of magnitude in the present flux model, any statistical relation between mass and velocity is of considerable interest. Velocity information is available only for photographic and radio meteors, both of which involve selection effects which lead to biased samples. Photographic data are more accurate, but the recently published data (Hawkins and Southworth [15 and 19]) contain values for the masses of meteoroids computed on Hawkins' [20] conventional model of the single-body meteor. More recent opinion discounting that any appreciable percentage of such substantial bodies are represented in photographic data was discussed in Section V.

In an analysis not yet published, the author derived the following formula for the mass of dustballs, based on Öpik's [11, 17] physical theory, on Whipple's [2] estimate of the mass of the meteoroid which produces a zero-visual-magnitude meteor at a velocity of 30 kilometers per second (based on the ARDC Model Atmosphere, 1959 [12]), and on an adjustment due to the U. S. Standard Atmosphere, 1962 [13]:

$$\log m = 1.40 + \log (h_B - h_e) - \log \cos Z - 2 \log v + 0.23 \sin 5(\log v - 1.55)$$

$$- (0.15 + 0.14 \log v) M_p \pm 0.30, \qquad (5)$$

where $h_B$ is the meteor height in kilometers above sea level at the point of appearance, $h_e$ is the meteor height in kilometers above sea level at the point of disappearance, Z is the angle to the meteor radiant, v is the meteoroid velocity before deceleration in the atmosphere, and $M_p$ is the meteor absolute photographic magnitude. Values for log m were obtained by equation (5) for each of the 285 meteors common to the two tables of data for random samples of sporadic meteors published by Hawkins and Southworth [15, 19]. The range for log m was

$$-2.2 \leq \log m \leq 1.0$$

with a mean for log m of -1.0. A multivariate statistical analysis was made for relating log m to log v, the absolute value of the celestial

latitude of the corrected radiant, the absolute value of the elongation of the true radiant from the apex of the earth's way and the heliocentric eccentricity of the orbit of the meteoroid. The following weighting function f was applied, hopefully to reduce the bias due to selection effects:

$$f \sim h_m^{-2} \, v^{-3/2} \, P^{-1} \, f_f \, e^{0.225Z} , \qquad (6)$$

where $h_m$ is the meteor height above sea level at the point of maximum brilliance, P is Öpik's (see Whipple [21]) probability that a meteoroid in a given orbit will encounter the earth during one revolution of the particle, $f_f$ is the reciprocal of the apparent fraction of the circle of celestial latitude through the meteor radiant, and e is the base of natural logarithms. Weighting the data had the following result relative to the corresponding analysis with uniform weight:

(1) The multiple correlation coefficient was increased from 0.161 to 0.319.

(2) The partial correlation coefficient with respect to log m and log v was increased from 0.033 to 0.101. The mean value of log v was decreased from log 29.3 to log 26.7.

Because the mass varies through only three orders of magnitude in the sample, and because the partial correlation coefficient with respect to log m and log v is small and likely not significant, it does not seem practical to try to establish a different mean velocity for meteoroids with smaller mass. However, it does appear likely that the lower weighted mean velocity may be a more nearly representative value for the model; i.e.,

$$\log v = \log 26.7 \pm 0.12. \qquad (7)$$

VII. MEAN FLUX FOR AN ORBITING VEHICLE

When the exposure circumstances (vulnerable area, etc.) for a vehicle in orbit do not vary during the orbital period, the expected number of impacts in an orbital period is the product of the orbital period, the area, and the orbital mean of the flux $\bar{F}_s$. Then by equation (1),

6

$$\log \bar{F}_s = \bar{\beta}_2 \log m + \beta_3, \tag{8}$$

where $\bar{\beta}_2$ is the orbital mean of $\beta_2$ in equation (2) and is approximated closely enough by the mean of the values of $\beta_2$ at perigee height $h_p$ and at apogee height $h_a$ - for orbits with low eccentricity - i.e.,

$$\bar{\beta}_2 = - \left\{ 1 + 0.17 \left[ e^{0.26(\log h_p - 2)} + e^{0.26(\log h_a - 2)} \right] - 0.12 \, (\log h_p h_a - 4) \right\} \tag{9}$$

$$= - \left[ 1 + 0.1011 \, (h_p^{0.11292} + h_a^{0.11292}) - 0.12 \, (\log h_p h_a - 4) \right]. \tag{10}$$

Hastings [8] gives the measured values of perigee height $h_p$ and apogee height $h_a$ for the Explorer XVI micrometeoroid satellite as 750 and 1180 kilometers, respectively. Then, by equation (10),

$$\bar{\beta}_2 = - 1.205. \tag{11}$$

## VIII. EXPECTED PUNCTURE FLUX

In Dalton's [7] model for the puncture of a homogeneous metallic wall by hypervelocity impact of a spherical projectile, the relation between the minimum sufficient mass m of the projectile, its velocity v, and angle of impact $x_2$ can be expressed as

$$\log m = - 1.9 + \log (p^3 \, \rho_t \, H_t) - (3/2) \, (\log v + \log \cos x_2) - \log \rho_p, \tag{12}$$

where $\rho_p$ is the projectile density and where $\rho_t$, $H_t$, and p are the density, hardness in Brinell units, and thickness in centimeters, respectively, for the punctured wall. For meteoroid impact onto a randomly oriented surface, the impact angle $x_2$ has sin $2x_2$ probability density. Then log m in equation (12) is a linear function of the three statistically independent random variables: $\log v$, $\log \rho_p$, and $\log \cos x_2$.

The mean of such a linear function is the function of the means; i.e.,

$$\log \bar{m} = -1.9 + \log (p^3 \, \rho_t \, H_t) - (3/2)(\log \bar{v} + \log \cos \bar{x}_2) - \log \bar{\rho}_p.$$

$$(13)$$

In Sections V and VI, reasons were discussed for considering $\log v$ and $\log \rho_p$ as essentially normally distributed. The weighted means and standard deviations according to equations (4) and (7) are

$$\log \bar{\rho}_p = \log 0.44 = -0.35 \tag{14}$$

$$\sigma_{\log \rho_p} = 0.30/0.6745 = 0.44 \tag{15}$$

$$\log \bar{v} = \log 26.7 = 1.43 \tag{16}$$

$$\sigma_{\log v} = 0.12/0.6745 = 0.18. \tag{17}$$

By integration, Dalton [7] showed that, for the other variable,

$$\log \cos \bar{x}_2 = -0.22 \tag{18}$$

$$\sigma_{\log \cos x_2} = 0.047. \tag{19}$$

The variance of a linear function of several statistically independent random variables is a linear function of the variances of the independent variables, the coefficients being the squares of the respective partial derivatives; i.e.,

$$\sigma^2_{\log m} = (3/2)^2 \, \sigma^2_{\log v} + (3/2)^2 \, \sigma^2_{\log \cos x_2} + \sigma^2_{\log \rho_p} = (0.52)^2.$$

$$(20)$$

8

Since a linear function of normal variables is also normal, and since the non-normal variable (log cos $x_2$) contributes less than two percent of the variance in equation (20), it follows that the logarithm of the minimum sufficient mass m in equation (12) is very nearly normally distributed. By equations (14), (16), and (18), the mean for this random variable is

$$\log \bar{m} = -3.36 + \log (p^3 \rho_t H_t).$$
(21)

By taking the differential of the antilogarithm of equation (1), the number of meteoroids $-dF_s$ impacting per square meter per second with masses between m and m + dm is

$$- dF_s = - 10^{\beta_3} \beta_2 m^{\beta_2-1} dm.$$
(22)

Then the number of punctures $\emptyset$ per square meter per second is

$$\emptyset = \int_{-\infty}^{\infty} -10^{\beta_3} \beta_2 P_m m^{\beta_2-1} dm,$$
(23)

where $P_m$ is the probability that the mass m of a meteoroid is sufficient for puncture (i.e., $P_m$ is the cumulative distribution of the normally distributed variable log m as defined by equations (12), (20), and (21)). The tangent line at the point $P_m = 1/2$ for the curve relating $P_m$ and log m is a very close approximation to the curve in the interval $0.25 \leq P_m \leq 0.75$, and its extension throughout the interval $0 \leq P_m \leq 1$ is close enough for the present purpose; i.e.,

$$P_m = 0 \qquad \text{for } m < 10^{\log \bar{m} - \frac{\sqrt{2\pi}}{2} \sigma_{\log m}},$$

$$= 1 \qquad \text{for } m > 10^{\log \bar{m} + \frac{\sqrt{2\pi}}{2} \sigma_{\log m}},$$
(24)

$$= (2\pi)^{-1/2} \left[ \frac{\log m - \log \bar{m}}{\sigma_{\log m}} \right] + \frac{1}{2}, \quad \text{otherwise}$$

Expected puncture fluxes $\emptyset_1$ and $\emptyset_2$ for the one-mil and two-mil respective thickness of beryllium copper on Explorer XVI will be determined. Hastings [8] showed that the one-mil and two-mil targets had mean thickness in excess of nominal thickness by 15 and 7.5 percent, respectively, and that the beryllium copper should be equivalent to targets of twice those thicknesses of 2024-T3 aluminum. Reismann, Donahue, and Burkitt [10] give the following values for the density $\rho_p$ and hardness $H_t$ of 2024-T3 aluminum: 2.77 and 120, respectively. Then, by equations (20-21), (23-24), (3) and (11) the puncturing mass and flux for those two targets should have been

$$\log \bar{m}_1 = -7.539 \tag{25}$$

$$\log \emptyset_1 = -4.562 \tag{26}$$

$$\log \bar{m}_2 = -6.727 \tag{27}$$

$$\log \emptyset_2 = -5.528. \tag{28}$$

The values for the puncture flux in equations (26) and (28) are 0.577 order of magnitude higher than the values of the impact flux by equations (8), (11), and (3) corresponding to the values for mass in equations (25) and (27), respectively. It should be expected that the 0.577 order of magnitude increment in the puncture flux (relative to the values which would be inferred from mean velocity, mean density, and mean impact angle) would have been slightly higher if $P_m$ had not been linearly approximated by equation (24) – say, 0.60. Hastings [9] gave the time-area product as $10^{7.06032}$ square meter seconds (1431 square foot days) after 44 punctures in the one-mil sensor and as $10^{6.7383}$ square meter seconds (682 square foot days) after 11 punctures in the two-mil sensor. With the puncture rates from equations (26) and (28), the predicted number of punctures would have been 315 and 16, respectively.

Hawkins and Upton [14] established the cumulative flux of meteors with respect to absolute photographic magnitude. If the mean velocity is assumed for all meteoroids, then a cumulative flux with respect to mass can be derived which is 0.65 order of magnitude lower than the one which Hawkins and Upton [14] gave and which is basic to the present model. In an analysis not yet completed, the author is investigating this effect with Hawkins' and Southworth's [15] random sample of 285 sporadic meteors.

# IX. PREFERRED MODELS FOR IMPACT AND PUNCTURE FLUX

The relation between the predicted number of punctures (315 and 16)* and the counted number (44 and 11) for the one-mil and two-mil sensors, respectively, over the same interval of the Explorer XVI flight, represents an agreement as close as one should expect by extrapolation from then existing observatory and laboratory data. But it should be expected that Explorer XVI results can be used to revise the puncture flux model for more accurate prediction of the puncture flux in cislunar space through walls of different material, thickness, and location. Because the number of punctures (44 and 11) is statistically a small sample in consideration of the extreme diversity of the population of incident meteoroids, and because the thicknesses of the two sensors differed only by a factor two, it seems appropriate to consider that the difference between the ratio of the predicted punctures (315:16) and the ratio of counted punctures (44:11) may be spurious. This provision is retained by reducing the impact and puncture flux in this new model by the weighted factor $10^{-\beta_4}$, where

$$\beta_4 = \frac{44 \, \log \, (315/44) + 11 \, \log \, (16/11)}{44 + 11} = 0.72. \qquad (29)$$

This adjustment is equivalent to substituting 60 and 3 for the counted punctures 44 and 11, respectively. Also, by the results of the examples in Section VIII, when log m in equation (1) is replaced by log $\bar{m}$ and an increment $\beta_5$ is added to the right, then log $F_s$ can be replaced by log $\emptyset$, where

$$\beta_5 = 0.60. \qquad (30)$$

Then, by equations (1), (3), (29), and (30), the incident flux $F_s$ and puncture flux $\emptyset$ can be found from

$$\log F_s = \beta_2 \log m - 14.92 \qquad (31)$$

$$\log \emptyset = \beta_2 \log \bar{m} - 14.32, \qquad (32)$$

where $\beta_2$ is given by equation (2) as a function of the distance h from the surface of the earth. But instead of substituting Dalton's [7] formula for log $\bar{m}$ in equation (21) into equation (32), it seems more

---

*Based on Pre-Explorer XVI results.

reasonable to derive a formula for log $\bar{m}$ from the results of the multi-variate statistical analysis of Reismann, Donahue, and Burkitt [10], and the result in equation (25) of applying equation (21) to the Explorer XVI conditions:

$$(\beta_2, \log p, \log \bar{m}) = (1.205, -2.233, -7.539), \tag{33}$$

where p is the thickness of 2024-T3 aluminum in centimeters.

Dr. O. K. Hudson, MSFC representative in the NASA Meteoroid Technology Advisory Working Group, recognized the pertinence of the effort by Reismann, Donahue, and Burkitt [10] and suggested Dr. Ezra's (Research Laboratories, Aerospace Division, Martin-Marietta Corporation) presentation of their preliminary results [10] at the Seventh Meeting of the NASA Meteoroid Technology Advisory Working Group, June 17-18, 1964. That effort involved a statistical analysis of available data from various sources for laboratory experiments with projectiles of various metallic materials impacting at various velocities at normal incidence into thick targets of various metallic materials. By maximizing the index of correlation of the hyperspatial regression surface with the experimental data, the best linear relation was sought between the logarithms of the crater-depth-versus-projectile-diameter ratio, of 9 physical and mechanical parameters of the target material, of the ratios of 13 corresponding projectile and target parameters, and of the ratio of the closing velocity to the bulk velocity of sound in the target material. Actually, the solution divided into three velocity regimes with linear segments having slopes of 1.206, 0.736, and 0.500 in the order of increasing velocity. Of the 22 independent variables which were investigated, seven were found sufficient to maximize the index of correlation. The results, with rounded off decimals, are as follows:

$$p_o/d = 7.0[(v/C_t)/(Q/Q_t)]^{1.21} (E/E_t)^{1.20} \epsilon_t^{0.51} \quad \text{low velocity} \tag{34}$$

$$= 5.4(v/C_t)^{0.74} (Q/Q_t)^{-0.89} (E/E_t)^{0.84} (\epsilon/\epsilon_t)^{-0.19} (Y_t/E_t)^{-0.10}$$
$$\text{intermediate velocity} \tag{35}$$

$$= 2.5(v/C_t)^{0.50} (E/E_t)^{1.31} (v/v_t)^{8.0} (\epsilon/\epsilon_t)^{0.43} \tag{36}$$
$$\text{high velocity}$$

where

$P_o$ = crater depth

d  = projectile diameter

v  = closing velocity in kilometers per second

t  = target subscript

$C_t$ = bulk velocity of sound in kilometers per second

Q  = Heat to melt in calories per gram

E  = $10^{-6}$ x Young's modulus, kilograms per square centimeter

$\epsilon$  = ductility, percent elongation in 2-inch gauge length at fracture

Y  = yield strength at 0.2 percent offset, kilograms per square centimeter

$\nu$  = Poisson's ratio.

The points of separation of the velocity regimes depend not only on the velocity, but also on the other parameters in equations (34-36) in a rather complicated manner which is described in Reference 10. Figures 1 and 2 compare these results with those for lines: (1) with slope 2/3 by Hermann and Jones [22] based on a survey and analysis of data and theory, and (2) with slope 1/2 previously suggested by Dalton [7] based on engineering judgment and a brief consideration of data and theory. Some of the data from Reference 10 extend up to about 8 kilometers per second, which velocity corresponds to the middle in Figures 1 and 2, and incidentally is the circular orbital velocity near the earth; but most of the data were at considerably lower velocities. The division of data into three velocity regimes is said [10] to have resulted in samples of from 100 to 170 data points in each regime. The multiple correlation coefficient with equations (34-36) was reported [10] to be 0.959, 0.982, and 0.989. As an alternative to equation (36), a more complicated formula involving a numerically small power of $Y_t/E_t$ increased the multiple correlation coefficient by 0.001, but equation (36) would seem to be appropriate.

Equation (36) cannot be used directly to establish a formula for log $\bar{m}$ in equation (32) because Young's modulus E, Poisson's ratio $\nu$, and ductility $\epsilon$ in equation (36) are hypothetical for dustball meteoroids. But it seems appropriate to consider the function of the projectile parameters in equation (36) as some undetermined constant. The diameter d of a spherical meteoroid is related to the mass m and density $\rho_p$ by

$$d = (6m/\pi\rho_p)^{1/3}. \tag{37}$$

FIGURE 1. RATIO OF CRATER DEPTH $p_o$ AND PROJECTILE DIAMETER d FOR IMPACT
OF SPHERICAL PROJECTILES OF SOFT ALUMINUM (HP Aℓ) AT
VELOCITY v KILOMETERS PER SECOND AT NORMAL INCIDENCE
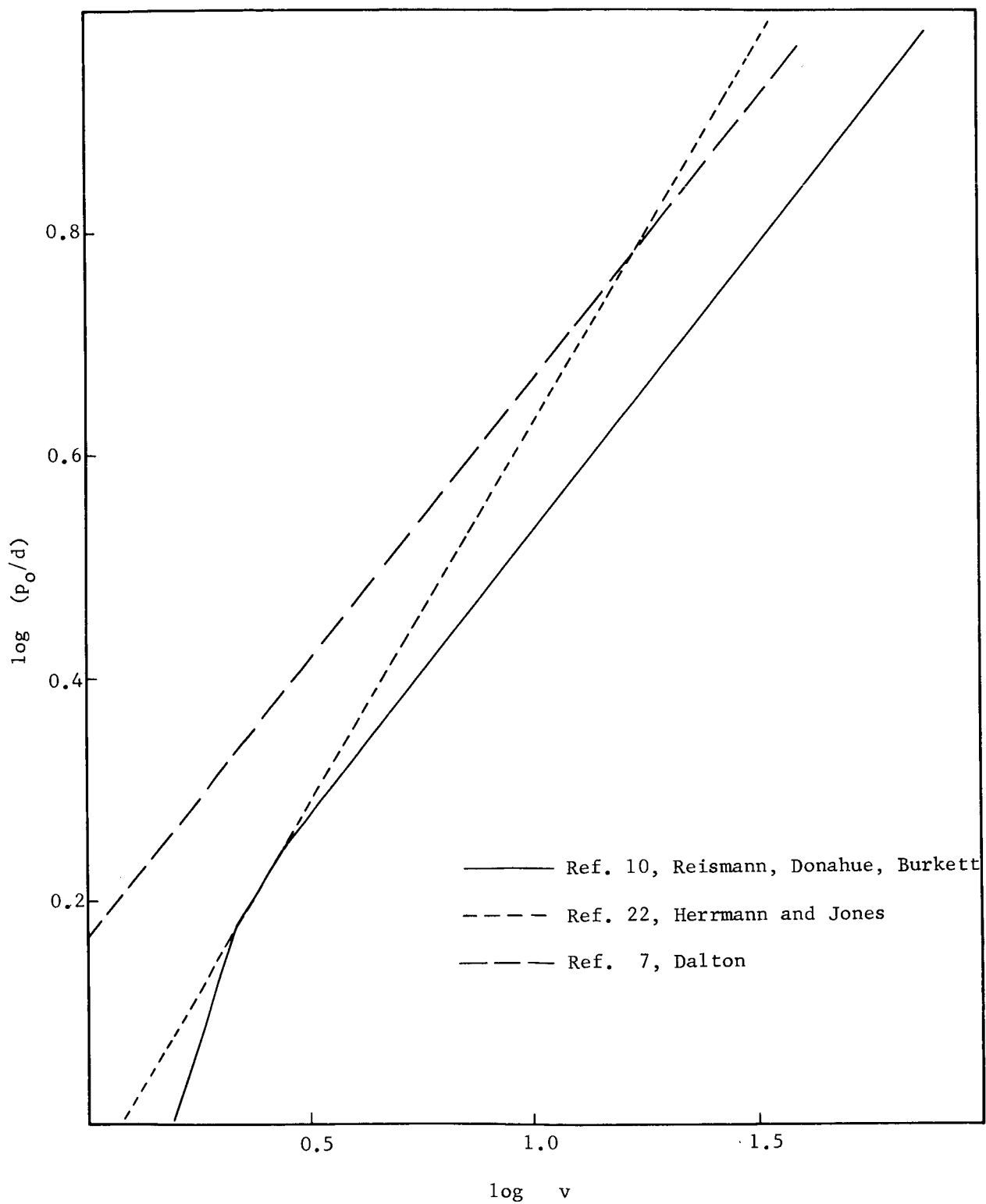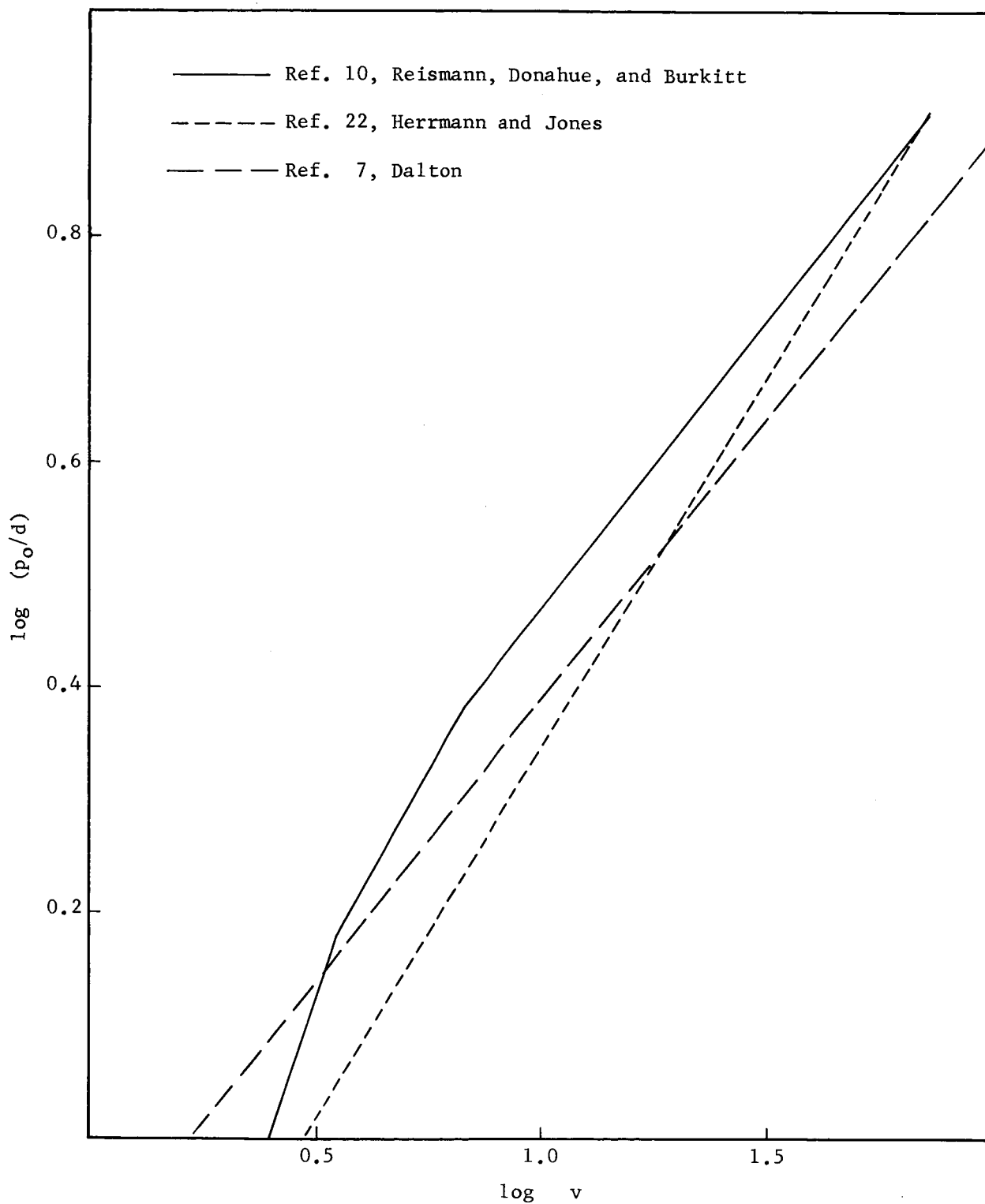ONTO THICK TARGETS OF SOFT ALUMINUM (HP Aℓ)

14

FIGURE 2. RATIO OF CRATER DEPTH $p_o$ AND PROJECTILE DIAMETER d FOR IMPACT OF SPHERICAL PROJECTILES OF HARD ALUMINUM (2024T-3) AT VELOCITY v KILOMETERS PER SECOND AT NORMAL INCIDENCE ONTO THICK TARGETS OF HARD ALUMINUM (2024T-4)

Also thick-target crater depth $p_0$ is thought (see Dalton [7]) to be proportional to the thickness $p$ of a just-puncturable wall. Therefore, equation (36) can be replaced by

$$\log \bar{m} = k + 3 \log(p C_t^{0.50} E_t^{1.31} v_t^{8.0} \epsilon_t^{0.43}), \qquad (38)$$

where $k$ is a constant. With the values for the material parameters in equation (38) tabulated in Reference 10, equation (33) can be supplemented for aluminum 2024-T3 as follows:

$$(\log p, \log \bar{m}, C_t, E_t, v_t, \epsilon_t) = (-2.233, -7.539, 6.25, \\ 0.745, 0.33, 0.18). \qquad (39)$$

Then, by equations (38) and (39), the constant $k$ in equation (38) can be evaluated, and equation (38) becomes

$$\log \bar{m} = 10.985 + 3 \log(p C_t^{0.50} E_t^{1.31} v_t^{8.0} \epsilon_t^{0.43}). \qquad (40)$$


X. PUNCTURE PREDICTION FOR THE PEGASUS EXPERIMENT


The Pegasus payload, described in References 23 and 24, is to be unfolded into a large randomly oriented winged orbiting structure instrumented to count meteoroid punctures. The Saturn SA-9 vehicle will be flown early in 1965 to insert a Pegasus payload into an orbit with perigee and apogee heights of 505 and 740 kilometers, respectively.[*] By equation (10), the value of $\beta_2$ in equations (31) and (32) is -1.229.

The unfolded Pegasus structure supports 416 flat metal sheets backed with puncture-sensing capacitors, each with a hemispherically exposed area of 0.516 square meter (20 by 40-inch rectangles). The 416 sensors are of three types, which will be called thin, thick, and thicker, and there are 16, 34, and 366 of each, respectively. The thin sheet is of soft aluminum (1100-H14) nominally 0.0015-inch. The other sheets are of hard aluminum (2024-T3) nominally 0.008 and 0.016-inch. The exposed surface of each sheet is coated with a layer of from 0.4 to 0.5 gram per square foot of MTL-3.[**] A 0.0005-inch trilaminate of mylar is attached to the back of each sheet with a 0.00018-inch layer of adhesive. The specific gravity of the mylar is 1.395. The density of the proprietary adhesive (G. T. Schjeldahl Co., Northfield, Minn.) has not been indicated;

---

[*] See footnote on page 19.

[**] Thermal Control Coating.

16

but a general rule for adhesives which is sufficiently accurate for this purpose is that the weight in pounds per square foot is about ten times the thickness in inches, and this would indicate a specific gravity of about 1.9. The thin sheet is bonded to the trilaminate of mylar by rolling, which is expected to dissipate most of the adhesive between the aluminum sheet and the trilaminate; but the other sheets are not rolled in applying the trilaminate. After the sheet has been bonded onto one side of the trilaminate, adhesive is applied to the other side as a base for the vacuum deposited 0.000025-inch copper plate of the capacitor. Apparently, the added materials which must be punctured weigh as much as a 0.0004-inch or 0.0005-inch foil of aluminum, even when the adhesive between the trilaminate and the copper is ignored, and the increased weight for the thin sensor is thought to be somewhat less than that for the other sensors.

The description of the Pegasus sensors which was given above, and which is illustrated in Figure 3, is somewhat different from that given in References 23 and 24. No adequate documentation has been found for this description, and the present description is not as definitive as it should be for the present purpose. It is based partly on information obtained in conversation with personnel from Pegasus Project Office, Propulsion and Vehicle Engineering Laboratory, Research Project Laboratory, Astrionics Laboratory, Fairchild Hiller Company (prime contractor), and G. T. Schjeldahl Company (subcontractor). Not only the adhesive but also the bonding process is said to be proprietary. Also no information was found for the actual thicknesses of the aluminum sheets in contradistinction to nominal thicknesses.

In this analysis it will be assumed that all three of these composite structures have the same puncture resistance as homogeneous sheets of 0.0004-inch increased thickness of the same aluminum materials would have.* Then the values for $\bar{m}$ in equation (32), the masses of the nominally puncturing meteoroids, are found by substituting into equation (40) the values of the material parameters from Reference 10; i.e.,

$$\log \bar{m} = -0.894 + 3 \log p \qquad \text{for soft aluminum (1100-H14)}$$

$$= -7.843 \qquad \text{for the thin sensors}$$

$$= -0.839 + 3 \log p \qquad \text{for hard aluminum (2024-T3)}$$

$$= -5.852 \qquad \text{for the thick sensors}$$

$$= -4.980 \qquad \text{for the thicker sensors.}$$

---

*The 1.5-mil sensor is equivalent to 1.9-mil aluminum 1100-H14, the 8-mil sensor is equivalent to 8.4-mil aluminum 2024-T3, and the 16-mil sensor is equivalent to 16.4-mil aluminum 2024-T3.

Therefore, by equation (32), the logarithms of the puncture fluxes per square meter per second are -4.681, -7.128, and -8.200 for the thin, thick, and thicker sensors, respectively. Then, by considering the exposed areas, one predicts that the corresponding values for the mean number of punctures per day are 14.9, 0.113, and 0.103, and per year* are 5430, 41, and 38 for the thin, thick, and thicker sensors, respectively.

## XI.  CONCLUSIONS AND RECOMMENDATIONS

Whipple's [2] model for the near-earth mean flux of meteoroids incident onto a randomly oriented surface should be considered to indicate flux too high by 0.44 order of magnitude. This proposed adjustment corresponds to an increase of 0.08 order of magnitude to include the mean flux from showers, an increase of 0.27 order of magnitude to adjust for pressure differences between the ARDC Model Atmosphere 1959 [12] and the U. S. Standard Atmosphere 1962 [13], a decrease of 0.07 order of magnitude through a simplifying approximation, and a further decrease of 0.72 order of magnitude for a weighted comparison with Hasting's [9] puncture results for Explorer XVI and Dalton's [7] model for puncturable-wall thickness. The 0.27-order-of-magnitude adjustment due to a revision of the assumed atmospheric pressure corresponds to a 0.20-order-of-magnitude increase in the assumed mass of the meteoroid at 30 kilometers per second velocity which produces a zero-absolute-visual-magnitude meteor (here revised to $10^{0.20}$ grams).

Whipple's [2] estimate of 0.44 gram per cubic centimeter for the mean density of meteoroids seems appropriate throughout the ten orders of magnitude below unit mass in grams. Over this range of mass, which is presupposed in this study, there is not sufficient evidence to indicate any significant statistical dependence between mass and velocity. The weighted mean and probable error of the logarithm of the geocentric velocity for photographic meteors are log 26.7 and 0.12, respectively; and the closing velocity with respect to an orbiting vehicle is not considered to be essentially different. But, because density, velocity, and impact angle are statistically independent random variables, the expected number of punctures through a given structure is four times as large as the expected number of incident meteoroids with mass equal to or greater than the mass of a meteoroid which will just puncture the structure when it has the mean velocity, the mean impact angle, and the mean density.

---

*See footnote on page 19.

At any fixed distance between one hundred and one million kilometers from the surface of the earth, meteoroid flux (incident flux or puncture flux) should be considered an exponential function of mass. The exponent has a unit negative value at the moon's distance, a value of $-1.34$ at one hundred kilometers above sea level, and an effective value of $-1.205$ for the Explorer XVI orbit. The incident flux $F_s$ and puncture flux $\emptyset$ are found from equations (31) and (32), respectively, when the value for the exponent $\beta_2$ is substituted from equation (2) and the value of the nominal mass $\bar{m}$ is substituted from equation (40).

During one year after a Pegasus satellite has been deployed in an orbit with perigee and apogee heights of 505 and 740 kilometers,* the number of punctures in the 16 sheets of the 0.0015-inch sensor, the 34 sheets of the 0.008-inch sensor, and the 366 sheets of the 0.016-inch sensor are predicted to be approximately 5430, 41, and 38, respectively,** when the extra material in the bonded capacitors is considered. The estimated masses of the meteoroids which can just puncture these sensors when they have the mean values of density (0.44 gram per cubic centimeter), velocity (26.7 kilometers per second), and impact angle ($\pi/4$ radian) are $10^{-7.84}$, $10^{-5.85}$, and $10^{-4.98}$ gram.

---

*These heights have been slightly revised recently in Reference 25.
** These numbers have not been adjusted for temporal changes in the orbital heights due to light pressure, aerodynamic drag, etc.
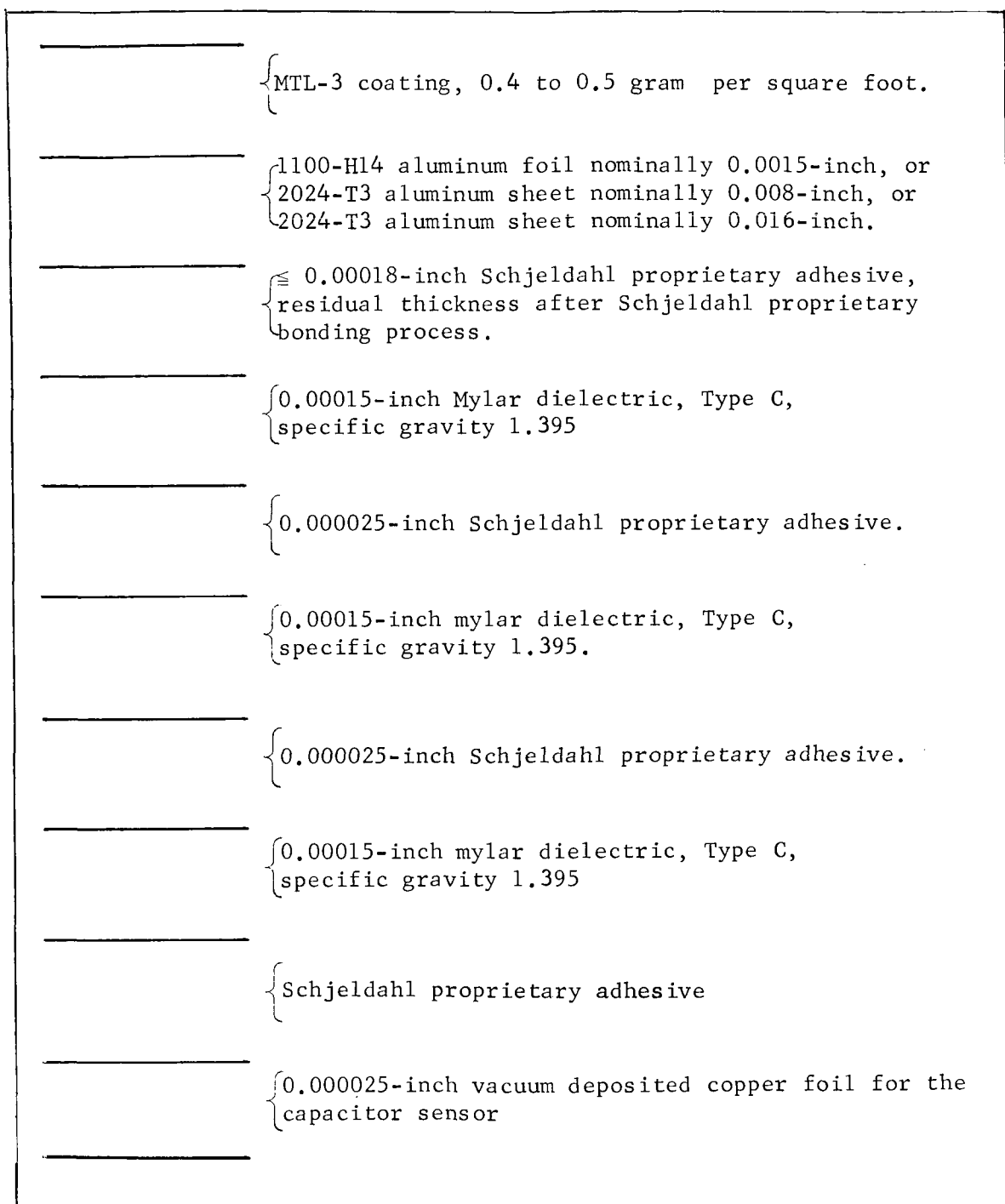
MTL-3 coating, 0.4 to 0.5 gram per square foot.

1100-H14 aluminum foil nominally 0.0015-inch, or
2024-T3 aluminum sheet nominally 0.008-inch, or
2024-T3 aluminum sheet nominally 0.016-inch.

≤ 0.00018-inch Schjeldahl proprietary adhesive,
residual thickness after Schjeldahl proprietary
bonding process.

0.00015-inch Mylar dielectric, Type C,
specific gravity 1.395

0.000025-inch Schjeldahl proprietary adhesive.

0.00015-inch mylar dielectric, Type C,
specific gravity 1.395.

0.000025-inch Schjeldahl proprietary adhesive.

0.00015-inch mylar dielectric, Type C,
specific gravity 1.395

Schjeldahl proprietary adhesive

0.000025-inch vacuum deposited copper foil for the
capacitor sensor

FIGURE 3. SCHEMATIC CROSS-SECTION FOR THE 10-LAYERED
CAPACITOR PUNCTURE SENSORS ON THE PEGASUS SATELLITE
BASED ON BEST INFORMATION AVAILABLE

20

REFERENCES

1. Dalton, C. C., "A Meteoroid Flux and Puncture Model for Near-Earth and Cislunar Space," Aero-Astrodynamics Laboratory Research Review No. 1 for the Period January 1, 1964 through June 30, 1964, NASA Technical Memorandum X-53189, October 15, 1964.

2. Whipple, F. L., "On Meteoroids and Penetration," Journal of the Astronautical Sciences, Vol. X, No. 3, pp. 92-94, Fall 1963.

3. Whipple, F. L., "The Dust Cloud About the Earth," Nature Magazine, Vol. 189, No. 4759, pp. 127-128, January 14, 1961.

4. Hawkins, G. S., "Impacts on the Earth and Moon," Nature Magazine, Vol. 197, No. 4869, pp. 781, February 23, 1963.

5. Briggs, R. E., "Steady-State Space Distribution of Meteoric Particles Under the Operation of the Poynting-Robertson Effect," Astronomical Journal, Vol. 67, No. 10, pp. 710-723, December 1962.

6. McCracken, C. W. and M. Dubin, "Dust Bombardment on the Lunar Surface," NASA Technical Note D-2100, December 1963.

7. Dalton, C. C., "Estimation of Tolerance Limits for Meteoroid Hazard to Space Vehicles ...," NASA Technical Note D-1996, February 1964.

8. Hastings, E. C., Jr., "The Explorer XVI Micrometeoroid Satellite Description and Preliminary Results for the Period December 16, 1962 through January 13, 1963," NASA Technical Memorandum X-810.

9. Hastings, E. C., Jr., "The Explorer XVI ... Supplement III ...," NASA Technical Memorandum X-949, March 1964.

10. Reismann, H., J. D. Donahue, and W. C. Burkitt, "Multivariable Analysis of the Mechanics of Penetration of High Speed Particles," Interim Technical Progress Report No. NASA-CR-64-5 (1 April 1963-31 May 1964, Contract No. NAS 7-219, OART, NASA Hq.) June 10, 1964.

11. Öpik, E. J., "The Masses of Meteors," Memoires de la Société Royale des Sciences de Liége, 4th Series, No. 15, pp. 125-146, 1955.

12. Mizner, R. A., K. S. W. Champion and H. L. Pond, "The ARDC Model Atmosphere, 1959," Air Force Cambridge Research Center, Technical Report 59-267, Air Force Surveys in Geophysics No. 115, August 1959.

13. "U. S. Standard Atmosphere, 1962," National Aeronautics and Space Administration, United States Air Force, United States Weather Bureau, December 1962, Government Printing Office, Washington, D. C.

REFERENCES (Continued)

14. Hawkins, G. S. and E. K. L. Upton, "The Influx Rate of Meteors in the Earth's Atmosphere," Astronomical Journal, Vol. 128, pp. 727-735, 1958.

15. Hawkins, G. S. and R. B. Southworth, "The Statistics of Meteors in the Earth's Atmosphere," Smithsonian Contributions to Astrophysics, Vol. 2, No. 11, 1958, Smithsonian Institution, Washington, D. C.

16. Whipple, F. L. and G. S. Hawkins, "Meteors," Handbuch der Physik, Vol. 52, pp. 517-564, Springer-Verlag, Berlin, 1959.

17. Öpik, E. J., "Physics of Meteor Flight in the Atmosphere," Interscience Tracts on Physics and Astronomy No. 6, Interscience Publishers, Inc., New York, 1958.

18. Jacchia, L. G. and F. L. Whipple, "Precision Orbits of 413 Photographic Meteors," Smithsonian Contributions to Astrophysics, Vol. 4, No. 4, Smithsonian Institution, Washington D. C., 1961.

19. Hawkins, G. S. and R. B. Southworth, "Orbital Elements of Meteors," Smithsonian Contribution to Astrophysics, Vol. 4, No. 3, 1961, Smithsonian Institution, Washington, D. C.

20. Hawkins , G. S., "The Method of Reduction of Short Trail Meteors," Smithsonian Contributions to Astrophysics, Vol. 1, No. 2, pp. 207-214, Smithsonian Institution, Washington, D. C.

21. Whipple, F. L., "Photographic Meteor Orbits and Their Distribution in Space," The Astronomical Journal, Vol. 59, No. 6, pp. 201-217, July 1954.

22. Herrmann, W. and A. H. Jones, "Survey of Hypervelocity Impact Information," Aeroelastic and Structures Research Laboratory, Massachusetts Institute of Technology, Report No. 99-1, September 1961.

23. "Micrometeoroid Capsule Description," Fairchild-Hiller, Inc. Hagerstown, Maryland, July 6, 1964.

24. Quarterly Progress Report No. 6, "Pegasus Meteoroid Technology Satellite Program," Space Systems Div., Fairchild Hiller, Inc., October 1964.

25. Wittenstein, G., "SA-9 Preliminary Predicted Trajectory," NASA Technical Memorandum X-53176, December 10, 1964.

Other NASA Technical Memoranda on Natural Environment Studies published by the Aero-Astrophysics Office, Aero-Astrodynamics Laboratory, George C. Marshall Space Flight Center, Huntsville, Alabama

1. TM X-53003, "Proposed Solution to the Geomagnetic Anomalies in the Ionosphere," William T. Roberts, September 1963.

2. TM X-53009, "Directional Wind Component Frequency Envelopes, Cape Kennedy, Florida, Atlantic Missile Range," O. E. Smith and Glenn E. Daniels, February 1964.

3. TM X-53103, "Temperature Measurements Inside a Rawinsonde Balloon," George T. Norwood, February 1964.

4. TM X-53018, "Space Radiations: A Compilation and Discussion," W. T. Roberts, March 1964.

5. TM X-53021, "Directional Wind Component Frequency Envelopes, Santa Monica, California, Pacific Missile Range," O. E. Smith and Glenn E. Daniels, March 1964.

6. TM X-53023, "Terrestrial Environment (Climatic) Criteria Guidelines for Use in Space Vehicle Development, 1964 Revision," Glenn E. Daniels, March 1964.

7. TM X-53027, "Cape Kennedy Low Level Wind Study for September 23-25, 1963," Carroll Hasseltine, April 1964.

8. TM X-53037, "Interparameter Statistical Analysis of Surface Wind Speed, Total Opaque Cloud Cover, and Maximum Wind Speed Aloft at Cape Kennedy, Florida," O. E. Smith, Lawrence E. Truppi and Harold L. Crutcher, April 1964.

9. TM X-53040, "Atmospheric Environment for Saturn (SA-5) Flight Test," J. W. Smith, April 1964.

10. TM X-53062, "An Automated Model for Predicting Aerospace Density Between 200 and 60,000 km Above the Surface of the Earth," Robert E. Smith, June 1964.

11. TM X-53064, "Latest Wind Estimates from 80 km to 200 km Altitude Region at Mid-Latitudes," W. T. Roberts, June 1964.

12. TM X-53089, "Study of Sphere Motion and Balloon Wind Sensors," Paul B. MacCready, Jr. and Henry R. Jex, July 1964.

13. <u>TM X-53104</u>, "An Automated Model for Predicting the Kinetic Temperature of the Aerospace Environment from 100 to 60,000 km Above the Surface of the Earth," Robert E. Smith, August 1964.

14. <u>TM X-53115</u>, "Details of Wind Structure from High Resolution Balloon Soundings," Robert Stinson, A. J. Weinstein and R. E. Reiter, August 1964.

15. <u>TM X-53116</u>, "An Empirical Analysis of Daily Peak Surface Wind At Cape Kennedy, Florida, for Project Apollo," J. David Lifsey, August 1964.

16. <u>TM X-53118</u>, "Distribution of Surface Meteorological Data for Cape Kennedy, Florida," J. W. Smith, August 1964.

17. <u>TM X-53119</u>, "Preliminary Cape Kennedy Atmospheric Data for Nuclear or Toxic Particles Dispersive Studies (August 1962 - July 1963)," C. K. Hill, August 1964.

18. <u>TM X-53124</u>, "Lunar Environment: An Interpretation of the Surface of the Moon and Its Atmosphere," John R. Rogers and Otha H. Vaughan, September 1964.

19. <u>TM X-53125</u>, "Far-Field Sound Propagation as Related to Space Vehicle Static Testing," O. E. Smith and D. G. McBride, September 1964, (pending release for distribution).

20. <u>TM X-53132</u>, "Stability Conditions of the Lower Atmosphere and Their Implications Regarding Diffusion at Cape Kennedy, Florida," James R. Scoggins and Margaret B. Alexander, September 1964.

21. <u>TM X-53139</u>, "A Reference Atmosphere for Patrick AFB, Florida, Annual (1963 Revision)," O. E. Smith and Don K. Weidner, September 1964.

22. <u>TM X-53142</u>, "Space Environment Criteria Guidelines for Use in Space Vehicle Development," Robert E. Smith, September 1964.

23. <u>TM X-53147</u>, "An Ultra-Low Frequency Electromagnetic Wave Force Mechanism for the Ionosphere," W. T. Roberts and J. M. Boyer, October 1964.

24. <u>TM X-53167</u>, "The Martian Environment," Robert B. Owen, November 1964.

25. <u>TM X-53186</u>, "Radiosonde Automatic Data Processing System," Robert E. Turner and Richard A. Jendrek, December 1964.
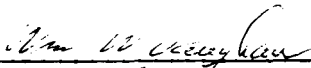
CISLUNAR METEOROID IMPACT AND PUNCTURE MODELS WITH
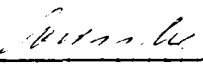PREDICTED PEGASUS SATELLITE PUNCTURES

By Charles C. Dalton


     The information in this report has been reviewed for security clas-
sification. Review of any information concerning Department of Defense
or Atomic Energy Commission programs has been made by the MSFC Security
Classification Officer. This report, in its entirety, has been deter-
mined to be unclassified.

     This document has also been reviewed and approved for technical
accuracy.




_____
W. W. Vaughan
Chief, Aero-Astrophysics Office




_____
E. D. Geissler
Director, Aero-Astrodynamics Laboratory

DISTRIBUTION

DIR
 Dr. von Braun
 Mr. Williams

DEP-T
 Dr. Rees

AST-S
 Dr. Lange

R-DIR
 Mr. Weidner
 Dr. McCall

R-SA
 Mr. Dannenberg
 Dr. Kuettner
 Dr. Shratter
 Mr. Wiley

R-FP
 Dr. Koelle
 Dr. Ruppe
 Mr. Ball
 Mr. Spears
 Mr. Huber

M-SSVH

MS-IP

MS-IPL (8)

MS-H

HME-P

CC-P

R-AERO
 Dr. Geissler
 Mr. Jean
 Mr. Larsen
 Mr. Cummings
 Mr. Dickey
 Dr. Heybey

R-AERO (Cont'd)
 Mr. Lavender
 Mr. Murphree
 Mr. Reed
 Dr. Sperling
 Mr. Dahm
 Mr. Holderer
 Mr. Huffaker
 Mr. J. Ballance
 Mr. Horn
 Mr. Rheinfurth
 Mr. Harcrow
 Mr. Winch
 Mr. Lester
 Mr. Thomae
 Mr. Hart
 Dr. Speer
 Mr. Kurtz
 Mrs. McNair
 Mr. Baker
 Mr. Fine
 Mr. Miner
 Mr. Schmeider
 Mr. McNair
 Mr. Teague
 Mr. Ledford
 Mr. McQueen
 Mr. deFries
 Mr. Brown
 Mr. Belew
 Mr. Schaefer
 Mr. Dale Ruth
 Mr. W. Vaughan (5)
 Mr. O. Vaughan (3)
 Mr. Scoggins
 Mr. R. Smith (3)
 Mr. O. Smith
 Mr. Daniels
 Mr. Dalton (40)

R-ASTR
 Dr. Haeussermann
 Mr. Currie
 Mr. Paludan
 Mr. Powell
 Mr. Digesu
 Mr. White
 Mr. Boehm
 Mr. Decker

DISTRIBUTION (Continued)

R-COMP
  Mr. Bradshaw
  Dr. Arenstorf

E-DIR
  Mr. Maus

I-E-E
  Mr. Waite

I-DIR
  Mr. Hueter

I-SE-CH
  Dr. Mrazek
  Mr. Finzel

I-E-Q
  Mr. Bombara

R-P&VE
  Mr. Cline
  Mr. Hellebrand
  Dr. Lucas
  Dr. Gayle
  Mr. Cataldo
  Mr. Zoller
  Dr. Krause
  Mr. Darwin
  Mr. Swanson
  Mr. Burrows

R-QUAL
  Mr. Grau
  Mr. Chandler

R-RP-DIR
  Dr. Stuhlinger
  Mr. Heller
  Mr. Cannon

R-RP-J
  Mr. Downey
  Mr. Jones
  Mr. Duncan
  Mr. Wells

R-RP-N
  Dr. Shelton
  Mr. Stern
  Dr. Hale

R-RP-P
  Dr. Dozier
  Mr. Hembree
  Dr. Hudson
  Mr. Naumann
  Mr. Holland

R-RP-S
  Dr. Mechtly

R-RP-X
  Mr. Urban

R-RP-T
  Mr. Bensko

I-I/IB-MGR
  Col. James

I-I/IB-P
  Dr. Johnson
  Mr. Wallace
  Mr. Morton

I-V-MGR

I-V-S-IVB

RSIC Library (8)

Scientific & Tech. Info. Facility (25)
P. O. Box 5700
Bethesda, Md.
Attn: NASA Rep. (S-AK/RKT)

27

EXTERNAL DISTRIBUTION

Meteoroid Technology Advisory Working Group (20)
Attn:   Mr. C. D'Aiutolo (Code: RV-1)
        NASA Headquarters
        Washington, D. C.

Dr. W. B. Foster, Director
Manned Space Sciences Div.
OSSA
NASA Headquarters
Washington, D. C.

NASA Headquarters
Washington, D. C.
Attn:   Technical Info. Div. (2)
        Office of Manned Space Flight (2)
        Office of Advanced Research & Technology (2)
        Office of Space Sciences and Applications (2)

NASA - Langley Research Center (3)
Hampton, Virginia

NASA - Goddard Space Flight Center (3)
Greenbelt, Md.

NASA - Lewis Research Center (3)
Cleveland, Ohio

NASA - Ames Research Center (3)
Moffett Field, Calif.

NASA - Manned Spacecraft Center (3)
Houston 1, Texas

NASA - Institute for Space Studies (3)           Air Force Cambridge Research
475 Riverside Dr.                                Laboratories (3)
New York 27, New York                            Bedford, Mass.

Jet Propulsion Lab. (3)                          Astrophysical Observatory (3)
4800 Oak Grove Dr.                               Smithsonian Institution
Pasadena, Calif.                                 Cambridge, Mass.

Bellcomm, Inc. (2)
1100 Seventeenth St., N. W.
Washington, D. C.